Cement & Concrete Composites 33 (2011) 246–250

Contents lists available at ScienceDirect

Cement & Concrete Composites

journal homepage: www.elsevier.com/locate/cemconcomp

Adsorption of methylene blue as a descriptor of C–S–H nanostructure

James J. Beaudoin *, Bussaraporn Patarachao, Laila Raki, Rouhollah Alizadeh

Institute for Research in Construction, National Research Council, Ottawa, Ontario, Canada K1A0R6

ARTICLE INFO

Article history:
Received 23 January 2009
Received in revised form 13 October 2010
Accepted 14 October 2010
Available online 13 November 2010

Keywords:
Methylene blue
Calcium silicate hydrate (C–S–H)
UV–VIS spectroscopy
Nanostructure

ABSTRACT

The adsorption of methylene blue (MB) on C–S–H surfaces (C/S ratios 0.60–1.80) and its dependence on C–S–H nanostructure was investigated. UV–VIS spectroscopy was used to obtain the adsorption–desorption isotherms at 23 °C, 35 °C and 50 °C. The character of the UV–VIS spectra and the nature of the C–S–H–MB interaction are discussed. Several sorption models including those due to Langmuir, Harkins–Jura, Halsey, Henderson, and Freundlich are fitted to the data using a non-linear multiple-regression method. Factors influencing the sorption of MB by C–S–H are discussed. The results demonstrated that the adsorption of MB molecules on C–S–H strongly depends on the nanostructural characteristics of C–S–H.

1. Introduction

Calcium silicate hydrate (C–S–H) is the principal binding phase in Portland cement-based products [1]. The behavior and performance of C–S–H in various environments is dependent on its chemical and physical stability and is central to sustainability issues [2]. The stoichiometry of C–S–H is variable and the C/S ratio generally ranges from 0.80 to 1.60 in cement systems (utilizing Portland or blended cements) hydrated at normal temperatures [3].

Recent studies motivated by sustainability objectives include the development of organic/inorganic cement-based nanoparticles [4–6]. These structurally modified materials often exhibit increases in the degree of polymerization of the silicate chains that form the backbone of their structure. The authors have demonstrated (using ^{29}Si NMR and XRD techniques) that when methylene blue (MB) solution interacts with C–S–H surfaces the effective silicate chain length increases [7]. The interaction of MB with smectites and other layered silicates has been studied extensively [8–10]. This investigation addresses whether or not the behavior of MB adsorption on C–S–H surfaces is analogous to sorption on clay surfaces. In this context the following objectives would appear to be relevant: to determine the efficacy of UV–VIS spectroscopy for the study of MB–C–S–H interactions; to establish if MB adsorption can form the basis for the development of a simple method for characterizing C–S–H preparations with variable C/S ratio; to validate the applicability of various sorption models to quantify the adsorption of MB on C–S–H surfaces and to clarify the factors that influence MB adsorption on C–S–H surfaces e.g. nanostructural variation, surface area. Details of this investigation are reported in the following sections.

2. Experimental

2.1. C–S–H preparation

C–S–H samples with C/S ratios of 0.60, 0.80, 1.00, 1.20, 1.40, 1.50, 1.60, 1.65, and 1.80 were prepared. Stoichiometric amounts of CaO and amorphous silica mixed with water at a water/solids ratio of about 11.80 were used to prepare samples with C/S ratio varying from 0.60 to 1.60. The preparations with C/S ratios 1.65–1.80 were prepared with stoichiometric amounts of CaO and amorphous silica corresponding to initial C/S ratios of 1.70 and 2.00. These samples contained significant amounts of free lime and the C/S ratios were corrected accordingly. The CaO was produced using precipitated calcium carbonate heated at 900 °C for 24 h. The CaO was purged with nitrogen gas and stored in a desiccator until required. The amorphous silica (Cabosil) was heated at 110 °C to dry the material thoroughly. The reactants for producing C–S–H were placed in high density polyethylene (HDPE) bottles that were continuously rotated for periods up to one year. The reaction temperature was 23 °C. The material was then filtered to remove excess water and dried under vacuum for 4 days. The resulting products were placed in HDPE bottles, purged with nitrogen gas and stored until further use. Samples of the various C–S–H preparations were put aside for immediate characterization using thermogravimetric analysis (TGA) and X-ray diffraction (XRD) methods.

* Corresponding author. Tel.: +1 613 993 6749; fax: +1 613 954 5984.
E-mail address: jim.beaudoin@nrc.ca (J.J. Beaudoin).

0958-9465/$ - see front matter Crown Copyright © 2010 Published by Elsevier Ltd. All rights reserved.
doi:10.1016/j.cemconcomp.2010.10.011

2.2. Characterization of C–S–H

TGA: The various C–S–H samples (10 mg) were placed in a TAQ 600 TGA instrument and heated at rate of 10 °C per min from room temperature to 1050 °C. The analysis was conducted in a nitrogen environment. The thermogravimetric curves (mass loss versus temperature) for the C–S–H preparations (C/S ratio of 0.80–1.60) were quantitatively and qualitatively similar to that reported for the C–S–H gel [11]. The mass loss in the region 400–600 °C was very small for the latter. An even smaller loss was observed for the C–S–H used in this study, suggesting that the residual amount of $Ca(OH)_2$ is small or negligible. Constitutional water loss likely contributes to the small mass loss in this region. This is not the case for the preparations having initial C/S ratios of 1.70 and 2.00 (corrected to C/S ratios of 1.65–1.80) due to the free lime that they contained.

XRD: The XRD measurements were performed with a Scintag XDS 2000 diffractometer using Cu Kα radiation. Characterization of the C–S–H was carried out in the range $5° < 2\theta < 60°$ using a continuous scan rate of 2°/min. A background correction was performed on the XRD patterns. The X-ray patterns indicated the presence of the primary peaks previously reported for C–S–H [3].

2.3. UV–VIS spectroscopy

UV spectrophotometric techniques were used to study the adsorption of MB cationic dye on the various C–S–H surfaces. These techniques have been successfully used in clay science investigations [10]. A Varian (Cary 5E) UV–VIS–NIR spectrophotometer was employed for this purpose. A UV–VIS calibration curve for aqueous MB solutions was constructed using concentrations of 1, 5, 10, 15 and 20 mg/L MB. Linear calibration curves can be constructed based on peak heights at each wavelength where a peak occurs. The solutions were kept in the dark to avoid photo degradation. The spectra for the MB solutions exhibit a strong absorbance peak at 664 nm with another peak on the shoulder at about 610 nm (Fig. 1). The absorbance at both 664 and 610 nm show a linear dependence with MB concentration.

2.4. C–S–H sorption experiments

An amount of 1.5 g of each C–S–H sample (C/S ratio: 0.60, 0.80, 1.00, 1.20, 1.50, 1.60, 1.65, 1.80) was weighed and mixed with 250 mL of MB solution (various concentrations) for 24 h. The mixtures were then centrifuged to separate C–S–H solids from the MB solution. The concentrations of the MB solutions after C–S–H treatment were determined using the UV spectroscopy. Sorption isotherms (adsorption and desorption) were constructed at 23 °C, 35 °C and 50 °C for the various C–S–H preparations.

3. Results and discussion

3.1. UV–VIS spectroscopy

The strong adsorption of MB onto the C–S–H samples was observed through the large decrease in the UV–VIS absorbance of the MB solution (15 mg/L) as shown for the preparations with variable C/S ratio in Fig. 2. The MB solution changed color from dark blue to light blue when in contact with the C–S–H samples. This is related to the metachromatic effect [12]. The change in color of the MB solution causes a shift in the UV–VIS absorption band. This phenomenon usually occurs when dye molecules are adsorbed or interact with materials such as polyelectrolytes, anionic polymers, and clay minerals [13,14]. Most authors explain this phenomenon in terms of formation of aggregates of dye molecules [15–17]. Each MB aggregation form absorbs light at different wavelengths as shown in Table 1.

In this study, the original MB solution (15 mg/L) shows a strong absorbance at 664 nm and a shoulder at about 610 nm indicating that the solution contains MB in the form of free monomers (MB^+) and free dimers $(MB^+)_2$ respectively. A shift in the absorbance peaks of the MB solutions towards lower wavelength numbers (for C–S–H with C/S ratio $\geqslant$ 1.0) was observed after the C–S–H samples were treated in MB solution for 24 h. This demonstrates that higher aggregations of MB molecules were formed in the solution. At high C/S ratios (C/S = 1.5, 1, 65 and 1.80) the MB solutions give very broad absorbance bands. These bands shift to

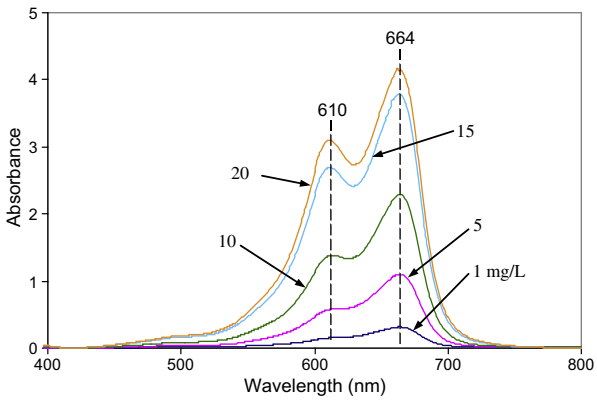

Fig. 1. UV–VIS spectra for MB solutions prepared at concentrations of 1, 5, 10, 15 and 20 mg/L.

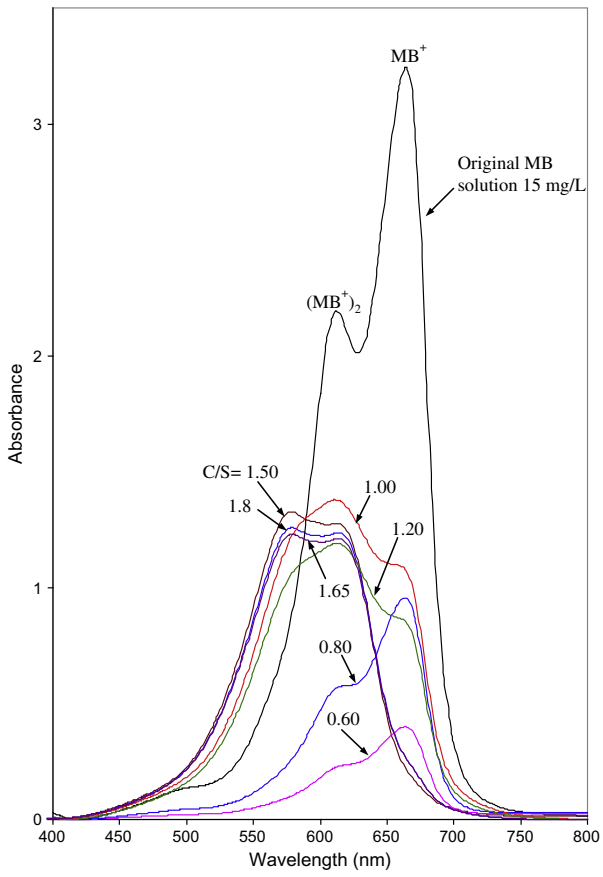

Fig. 2. UV–VIS spectra for C–S–H preparations (C/S ratio = 0.60–1.80) immersed in MB solutions.

Table 1
Characteristic UV bands of absorbed MB [11].

Wavelength (nm)	Species	Assignment
760	MBH^{2+}	Protonated MB
653–670	MB^{+}	Monomer
600–610	$(MB^{+})_2$	Dimer
570	$(MB^{+})_3$, $(MB^{+})_n$	Trimer and higher aggregates
720	$(MB^{+})_2$	L-dimer

≈610–570 nm showing that the solutions contain dimer, trimer and higher aggregates of MB molecules. The C–S–H specimens with C/S ratio = 0.60 and 0.80 have the greatest adsorption capacity and the highest values of nitrogen surface area (204 and 186 m^2/g respectively). Adsorption of MB for the specimens having C/S ⩾ 1.0 is significantly less and in the following order: C/S = 1.65 > 1.80 > 1.50 > 1.20 > 1.00. The nitrogen surface area values given in the same order are 49.0, 43.0, 52.0, 30.0, and 29.0 m^2/g. An argument could be made that if the C–S–H preparations with C/S ratio = 1.65, 1.80 and 1.50 are considered as a group (surface area values vary in a narrow range i.e. 43.0–52.0 m^2/g), that adsorption is dependent on surface area.

It is suggested that when MB molecules adsorb onto the C–S–H surface the cationic monomer and dimer species are initially adsorbed via cation exchange with Ca^{2+} onto anionic sites through an electrostatic attraction mechanism. This exchange is illustrated by the increase in pH of the MB solutions measured during the 24 h of interaction with the C–S–H samples. The pH of these solutions increases proportionally from about 10 to 12.5 (Fig. 3). Most of the increase occurs during the first hour. The rapid interaction between the MB solution and the C–S–H is clearly demonstrated in the UV spectra taken at intervals between 2 min and 24 h (Fig. 4). Consider the adsorption of MB onto C–S–H with C/S = 0.60. A large decrease in the intensity of the monomer and dimer bands was observed after the second minute of addition (Fig. 4a). A significant decrease in absorbance at 2 min can also be seen for the C/S = 1.20 preparation (Fig. 4b). A shift in absorbance toward lower wavelength numbers was observed after 24 h. At higher C/S ratios e.g. C/S = 1.80 (Fig. 4c) a shift toward lower wavelength numbers occurs after 2 h. The band is completely shifted after 24 h.

3.2. C–S–H–MB adsorption isotherms

Complete adsorption and desorption isotherms (obtained at 25 °C, 35 °C and 50 °C) were obtained for the C–S–H preparations

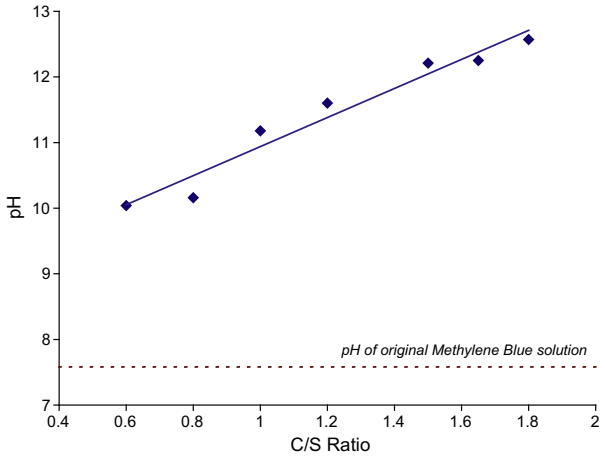

Fig. 3. pH values of MB solutions (15 mg/L) after immersion of C–S–H preparations (C/S ratio = 0.60–1.80) in the solutions.

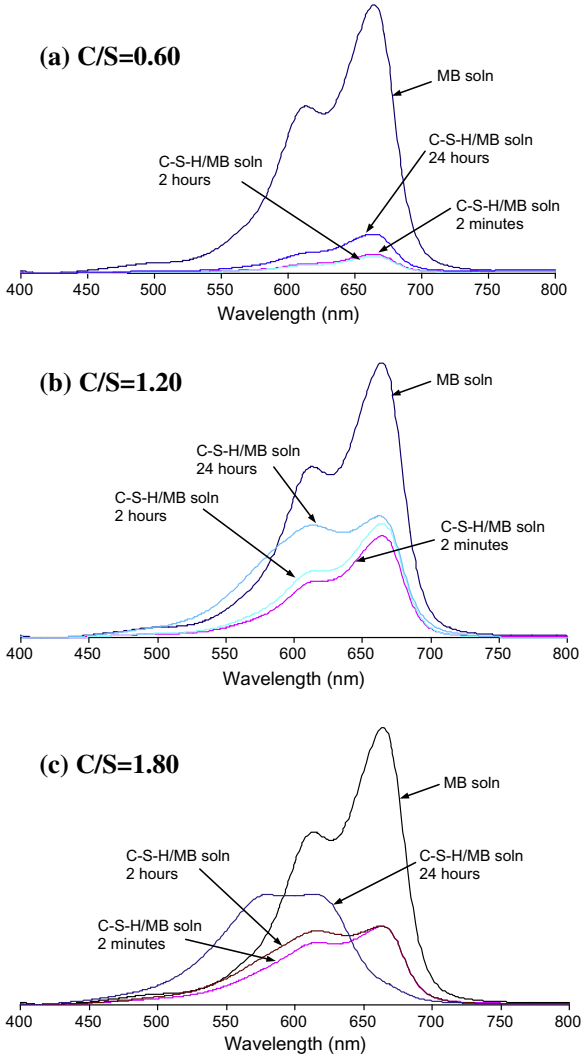

Fig. 4. UV–VIS absorption spectra of C–S–H in MB solution (15 mg/L) collected at 2 min, 2 h and 24 h compared with the original MB solution: (a) C/S = 0.60, (b) C/S = 1.20 and (c) C/S = 1.80.

with variable C/S ratio. Adsorption–solution concentration curves for C–S–H samples having C/S ratios of 0.80, 1.00 and 1.60 are shown in Fig. 5a–c respectively. A maximum concentration of 30 mg/L was included in the experiments. Examination of the data indicates that the adsorption results are very similar at all three temperatures up to a MB concentration level of 15 mg/L. This apparent temperature independence is likely related to the very strong affinity of the MB molecules for the C–S–H surfaces and the extremely rapid adsorption rate. At MB concentrations >15 mg/L adsorption at 35 °C exceeds that at 23 °C and 50 °C for C/S ratios = 0.80 and 1.00. The C/S ratio = 1.60 samples have the largest adsorption at 23 °C. Differences in the amount adsorbed at the three temperatures are relatively small for the C/S = 0.80 preparation. These differences are much larger at C/S = 1.00 and 1.60. The lack of a consistent temperature related trend between the different C/S ratio preparations may be due to C–S–H nanostructural differences. The latter occurring in C–S–H preparations having C/S ratio ⩾ 1.00 have been well documented [18]. The differences include a significant lowering in the degree of polymerization of the silicate sheets due to structural defects e.g. missing bridging tetrahedra. The ^{29}Si NMR evidence reported elsewhere [7] for C–S–H–MB nanomaterials suggests that increases in the Q^2/Q^1 ratio following adsorption of MB on C–S–H surfaces can be

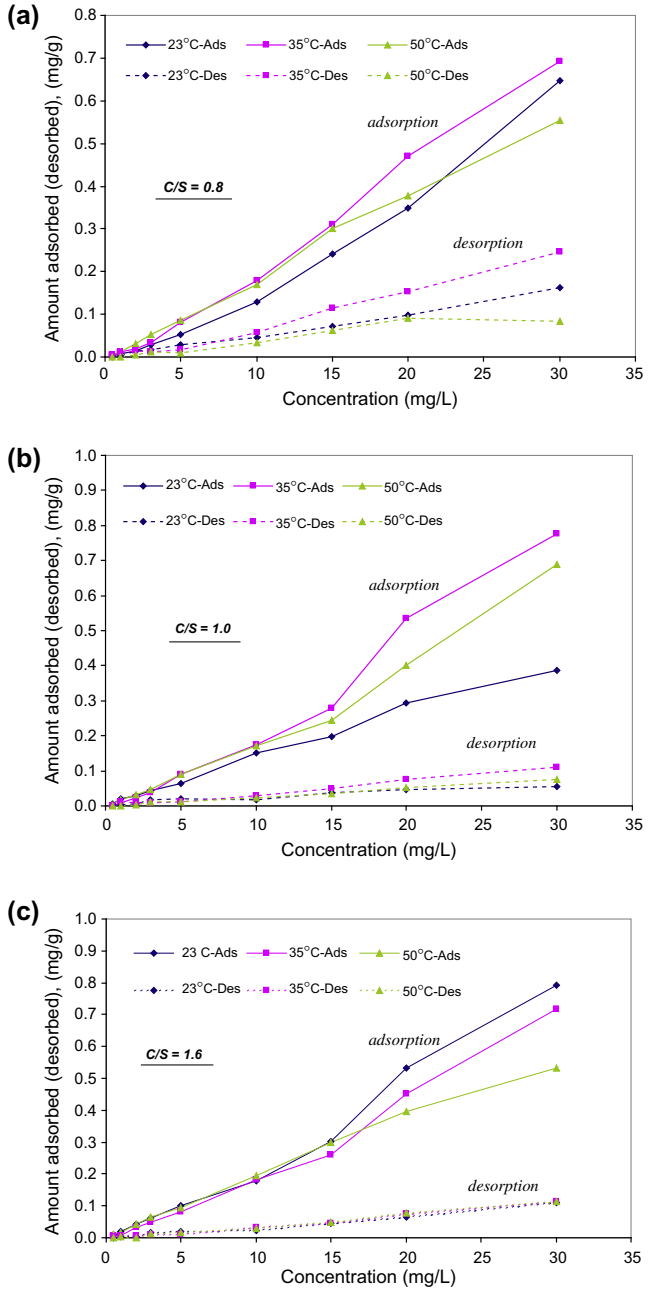

Fig. 5. Sorption–desorption isotherms for MB on C–S–H preparations (C/S ratio = 0.80, 1.00 and 1.60) at 23 °C (a), 35 °C (b) and 50 °C (c).

interpreted as a result of the adsorption of MB molecules at defect sites leading to an 'effective' increase in chain length. It is known that electrons of the atoms in the vicinity of existing –O–Si–O bonds can shield the silicon nuclei resulting in a detectable chemical shift. These shifts depend on the extent and strength of shielding. A chemical shift for the silicon atom will occur in the case of –O–Si–O–[Polymer]. The chemical shift of Si in the vicinity of the polymer can be similar to that obtained with a Si–O–Si bond and mimic the latter which is called Q^2. This effect is an indication that adsorption of MB on C–S–H surfaces may be both temperature and nanostructure dependent. Further study is required. The differences in surface area for the C–S–H preparations with C/S ratio $\geqslant$ 1.00 are not large suggesting that this parameter would only have a minor effect on amounts adsorbed. The significantly larger surface area would likely be a contributing factor to larger adsorption

Table 2
Constant parameters and correlation coefficients calculated for various adsorption models of MB adsorption on C–S–H (C/S = 1.60) at different temperatures.

Isotherm equation	Temperature (°C)	Constant parameters		R^2 (%)
Langmuir	23	$y_m = 2.32$	$k = 0.01$	99.8
$C/y = 1/ky_m + (1/y_m)C$	35[a]	$y_m = 0.44$	$k = 0.02$	88.0
	50	$y_m = 1.46$	$k = 0.01$	98.9
Harkins–Jura	23	$A = 228.10$	$B = 1.51$	85.3
$1/y^2 = (B/A) - (1/A)\ln C$	35	$A = 168.09$	$B = 1.51$	86.3
	50	$A = 177.59$	$B = 1.54$	82.2
Halsey	23	$n = 0.20$	$k = 3.36$	99.0
$\ln y = [(1/n)\ln k] - (1/n)\ln[\ln(1/C)]$	35	$n = 0.19$	$k = 3.30$	99.4
	50	$n = 0.25$	$k = 3.02$	98.6
Henderson	23	$n = 0.82$	$k = 0.04$	99.1
$\ln[-\ln(1-C)] = \ln k + n\ln y$	35	$n = 0.79$	$k = 0.04$	99.6
	50	$n = 1.00$	$k = 0.05$	99.9
Freundlich	23	$n = 1.24$	$k_f = 0.01$	99.1
$\ln y = \ln k_f + n\ln C$	35	$n = 1.28$	$k_f = 0.01$	99.6
	50	$n = 0.91$	$k_f = 0.02$	99.7

Note: for Halsey and Henderson, C was divided by 1000. For Harkins–Jura, y was multiplied by 100, y is the adsorption capacity of MB (mg/g); y_m is the monolayer adsorption capacity. C is equilibrium concentration; n, k, A, B, k_f are constant parameters for the isotherm equations.

[a] Negative values for the parameters.

at C/S ratios <1.00 but would appear to have little effect on the small variations due to temperature.

The amount of MB desorbed from the C–S–H surfaces is relatively small for all C/S ratios. At C/S ratios $\geqslant$1.00 the temperature effect is negligible and the amount of MB desorbed is <0.1 mg/g. At C/S ratios <1.00 the amount desorbed is slightly higher (although there is no direct temperature dependence) possibly due to the much higher surface area values and the higher total amount of MB adsorbed.

3.3. Sorption models for C–S–H–MB

A non-linear multiple regression procedure was applied to the adsorption data using several different adsorption models. Typical results using the data for C–S–H with C/S ratio = 1.60 are given in Table 2.

With the exception of the Harkins–Jura model all the models provide exceptionally good fits with correlation coefficients generally greater than 99%. This is consistent with observations of the adsorptive properties of the clay–water system [8]. The Harkins–Jura model appears to work better for clay systems than for C–S–H.

A major difference between clays and C–S–H is that the energetics of intercalation favors greater adsorption on the interlayer clay surfaces than in the C–S–H interlayer region. Clays, for example, can accommodate several layers of water molecules in the interlayer region. Only one layer of water molecules can reside in the C–S–H interlayer [19]. This can account for the large MB adsorption capacity of clays relative to C–S–H.

The Freundlich isotherm often represents an initial surface adsorption followed by a condensation effect resulting from extremely strong solute–solute interaction. This would appear to be the case for the interaction of MB with C–S–H surfaces since a significant amount of sorption occurs within 2 min. Sorption curves representing data for the C–S–H (C/S ratio = 1.60) preparation fitted to the Freundlich isotherm are provided in Fig. 6a–c. The excellent quality of the fit is apparent.

4. Conclusions

1. UV–VIS spectroscopy can be used to determine the sorption properties of C–S–H in MB solutions.

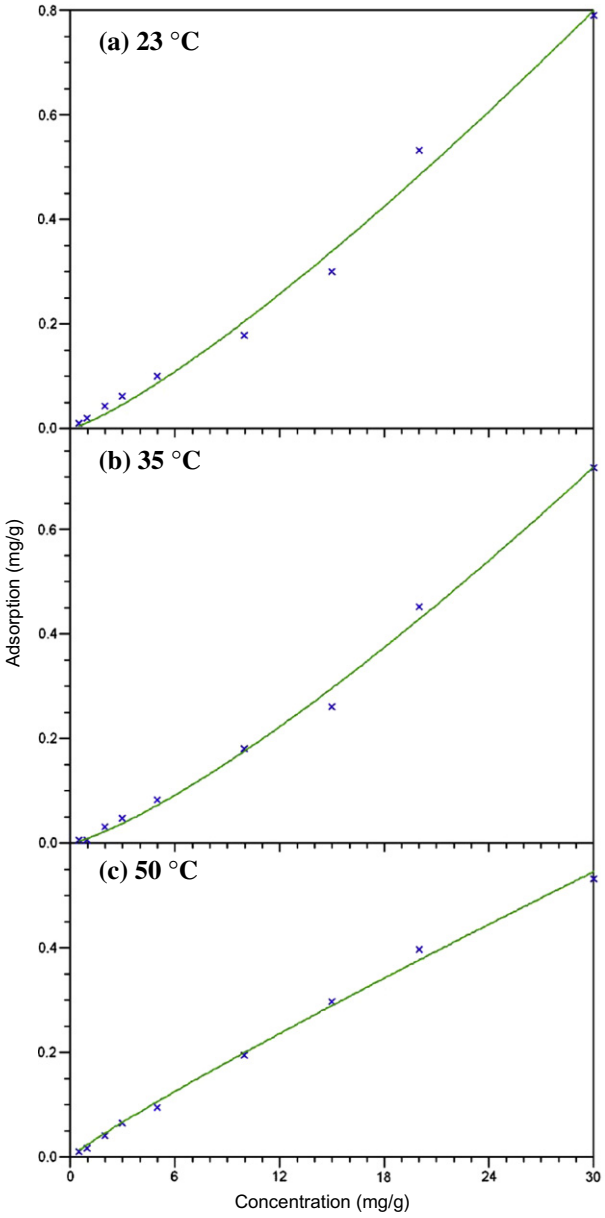

Fig. 6. MB sorption curves for C–S–H (C/S ratio = 1.60) obtained at 23 °C (a), 35 °C (b) and 50 °C (c). The data are fitted to the Freundlich model.

2. There is a strong and rapid interaction of MB with C–S–H surfaces. A significant amount of adsorption occurs in less than 2 min.
3. The character of the UV–VIS spectra for C–S–H immersed in MB solution is dependent on the C/S ratio. Higher aggregations of MB molecules are formed in solution when MB interacts with C–S–H having C/S ratio $\geqslant$ 1.00.
4. The total amount of MB adsorbed on C–S–H surfaces generally increases with nitrogen surface area and decreases with C/S ratio. It is suggested that MB adsorption could form the basis of a quick and simple test to estimate the surface area and approximate C/S ratio of C–S–H.
5. Interaction of MB solution with C–S–H surfaces may involve cation exchange with Ca^{2+} onto anionic sites by electrostatic attraction. This is accompanied by a rapid increase in the pH of the solution.
6. Adsorption of MB on C–S–H surfaces at solution concentrations up to 15 mg/L is not significantly influenced by temperature in the range, 23–50 °C. This may be related to the very strong affinity of the MB molecules for C–S–H surfaces as reflected by the extremely rapid rate of sorption at all temperatures in this range.
7. Adsorption of MB at solution concentrations >15 mg/L is influenced by bulk temperature and nanostructural variation i.e. degree of polymerization and the C/S ratio of the C–S–H.
8. The desorption branch of the MB sorption isotherm is relatively flat indicating the highly irreversible nature of the interaction of MB with the C–S–H surface.
9. Several sorption models e.g. Langmuir, Halsey, Henderson and Freundlich can be used to describe the adsorption of MB on C–S–H surfaces. This is consistent with the adsorptive properties of the clay/water system.
10. The higher sorption capacity of clay systems for MB relative to C–S–H systems can be explained by the energetics of the intercalation process that results in several layers of water molecules resident between clay layers as opposed to a single layer in the case of C–S–H.

References

[1] Taylor HFW. The Chemistry of cement hydration. In: Burke JE, editor. Progress in ceramic science, vol. 1. New York: Pergamon Press; 1960. p. 89–145.
[2] Ramachandran VS, Feldman RF, Beaudoin JJ. Concrete science. London: Heyden and Son; 1981.
[3] Taylor HFW. Cement chemistry. London: Thomas Telford; 1997.
[4] Raki L, Mojumdar SC, Lang S, Wang D. Spectral and microscopic properties of calcium silicate hydrate polymer nanocomposites. In: Proc. 12th Int. Congr. Chem. Cem. Theme ST5, Montreal; July 08 2007.
[5] Merlin F, Lombois H, Joly S, Lequeux N, Halay J-L, VanDamme H. Cement-polymer and clay-polymer nano and meso composites: spotting the differences. J Mater Chem 2002;12:3308–15.
[6] Franceschini A, Abramson S, Bresson B, VanDamme H, Lequeux N. Cement-polymer nanocomposites. In: Proc. 12th Int. Congr. Chem. Cem. Theme ST5, Montreal; July 08 2007.
[7] Beaudoin JJ, Patarachao B, Raki L, Alizadeh R. Interaction of methylene blue dye with calcium–silicate–hydrate. J Am Ceram Soc 2009;92(1):204–8.
[8] Gurses A, Karaca S, Dogar C, Bayrak R, Acikyildiz M, Yalcin M. Determination of adsorptive properties of the clay/water system: methylene blue adsorption. J Colloid Interf Sci 2004;269:310–4.
[9] Basar C. Applicability of the various adsorption models of three dyes: adsorption onto activated carbon prepared waste apricot. J. Hazard Mater 2000;B135:232–41.
[10] Jacobs K, Schoonheydt R. Spectroscopy of methylene blue–smectite suspensions. J Colloid Interf Sci 1999;220:103–11.
[11] Taylor HFW. Proposed structure for calcium silicate hydrate gel. J Am Ceram Soc 1986;69(6):464–7.
[12] Schoonheydt RA, Heughebaert L. Clay adsorbed dyes; methylene blue on laponite. Clay Miner 1972;27:91–100.
[13] Otsuki S, Adachi K. Metachromasy in polymer films. Changes in the absorption spectrum of methylene blue in nafion films by hydration. Polym J 1993;25:1107–12.
[14] Wohlrab S, Hoppe R, Schultz-Ekloff G, Worle D. Encapsulation of methylene blue into aluminophosphate family molecular sieves. Zeolites 1992;12:862–5.
[15] Breen C, Rock B. The competitive adsorption of methylene blue onto montmorillonite from binary solution with thioflavin T, proflavin and acridine yellow. Clay Miner 1994;29(12):179–89.
[16] Bergman K, O'Konski CT. A spectroscopic study of methylene blue monomer, dimer and complexes with montmorillonite. J Phys Chem 1963;67:2169–77.
[17] Azner AJ, Casal B, Ruiz-Hitzky E, Lopez-Arbeloa I, Santaren J, Alvarez A. Adsorption of methylene blue on sepiolite gels: spectroscopic and rheological studies. Clay Miner 1992;27:101–8.
[18] Cong X, Kirkpatrick RJ. ^{29}Si MAS NMR study of the structure of calcium silicate hydrate. Adv Cem Bas Mater 1996;3:144–56.
[19] Feldman RF. Assessment of experimental evidence for models of hydrated Portland cement. Highway Res Rec 1972;370:8–24.